agriculture

MDPI

Article

Climate Change Impacts on Surface Runoff and Nutrient and Sediment Losses in Buchanan County, Iowa

Edward Osei [1,*], Syed H. Jafri [2], Philip W. Gassman [3], Ali Saleh [4] and Oscar Gallego [4]

[1] Department of Agriculture Education and Communication, Tarleton State University, Stephenville, TX 76402, USA
[2] Department of Accounting, Finance, and Economics, Tarleton State University, Stephenville, TX 76402, USA
[3] Center for Agricultural and Rural Development, Iowa State University, Ames, IA 50011, USA
[4] Texas Institute for Applied Environmental Research, Tarleton State University, Stephenville, TX 76402, USA
* Correspondence: osei@tarleton.edu

Abstract: Nonpoint source pollution from cultivated croplands has often been associated with downstream water quality impairment in various watersheds. Given projected changes in global climate patterns, this study contributes to the existing literature by elucidating the impacts of climate projections on edge-of-field surface runoff and sediment and nutrient losses. We apply a well-tested ecohydrological model, Agricultural Policy Environmental eXtender (APEX), to continuous corn and corn–soybean fields in Buchanan County, Iowa, using climate scenarios developed from three well-known representative concentration pathway (RCP) climate projections: RCP 2.6, RCP 4.5, and RCP 8.5. Our results indicate that there will be a moderate to substantial increase in surface runoff, sediment, and nutrient losses depending upon the reference point of comparison (baseline scenario) and upon which climate scenario actually materializes. However, regardless of which climate scenario materializes and regardless of the baseline for comparison, soluble nitrogen losses are bound to increase, the magnitude depending upon the climate scenario. We find also that nutrient losses will be higher from continuous corn fields than from corn–soybean fields, given the tillage practices implemented on corn versus soybeans in the study area. Similarly, we find that nutrient losses may be higher from fields that receive manure than fields that receive only inorganic fertilizer, though this latter finding may be predicated upon the specific nutrient application rates utilized.

Keywords: climate change; sediment losses; nutrient losses; APEX; CMIP5; PRISM

Citation: Osei, E.; Jafri, S.H.; Gassman, P.W.; Saleh, A.; Gallego, O. Climate Change Impacts on Surface Runoff and Nutrient and Sediment Losses in Buchanan County, Iowa. *Agriculture* **2023**, *13*, 470. https://doi.org/10.3390/agriculture13020470

Academic Editor: Rabin Bhattarai

Received: 29 December 2022
Revised: 10 February 2023
Accepted: 15 February 2023
Published: 16 February 2023

1. Introduction

Surface runoff from agricultural fields has long been implicated for the water quality impairment of downstream rivers, lakes, and oceans [1–6]. Phosphorus losses are the primary concern from livestock impacted watersheds [7,8], while sediment and nitrogen loads are the main indicators of concern from cultivated croplands [9,10]. In response, agricultural producers and local, regional, and national government agencies across the world have made significant investments in conservation practices to minimize surface runoff and associated nutrient and sediment loads to downstream waterbodies [5].

While conservation practices have to some extent been effective at mitigating surface runoff losses, their overall performance has been partly uncertain for various reasons [11,12]. Among the key factors influencing the effectiveness of practice implementation is the prevailing weather. Various studies, e.g., [13–16], indicate that weather is a highly significant factor driving surface runoff and nutrient and sediment losses, as well as the effectiveness of the practices implemented to mitigate those losses.

Given the importance of weather patterns as a key driver for surface runoff losses and the effectiveness of mitigation efforts, it is vital to better understand the implications of future climate projections for resource conservation. A number of studies have indicated that future climate projections will result in the increased intensity of rainfall events,

e.g., [17,18], with resulting increases in surface runoff and sediment and nutrient losses [19–24]. Notwithstanding the attention given to the impact of climate change on surface runoff and nutrient and sediment losses from agricultural lands, a more comprehensive assessment applicable to cultivated cropland is lacking. For instance, what are the relative impacts of various rotations? What are the implications of utilizing manure nutrients versus inorganic fertilizer?

In this study, we contribute to the existing literature by assessing the impacts of future climate projections on corn and soybean production in a highly crop-intensive county in northeastern Iowa. We explore the implications of multiple climate scenarios in order to provide a broad perspective of the likely trajectory of nutrient and sediment losses regardless of which future climate scenario actually materializes. To this end, we utilize well-established crop management practices for that region, including the use of manure and inorganic fertilizers. To capture future climate patterns, we use the most widely accredited climate projections to determine the impacts of these climate forecasts on surface runoff and sediment and nutrient losses from continuous corn and corn–soybean fields in a predominantly cash crop-producing county in Iowa. The county chosen for this study—Buchanan County, Iowa—was selected because of previous extensive model calibration and validation efforts that produced a robust model capable of tracking edge-of-field runoff, sediment, and nutrient losses. The computer model we used to arrive at the impacts of the climate projections on the edge-of-field runoff and sediment and nutrient loss indicators was the Agricultural Policy Environmental eXtender (APEX) [25,26], a well-tested and calibrated ecohydrological model that has been widely applied in many contexts across the globe [27].

This study leverages previous work in northeast Iowa that entailed APEX and Soil and Water Assessment Tool (SWAT) [28] calibration and validation efforts [27,29]. A more recent study performed additional APEX validation tests for Buchanan County and used the model to simulate corn and soybean yields under projected climate change [30]. The results of APEX validation efforts indicate that the model is well suited for simulating not only crop yields but also the fate and transport of water, sediment, and nutrients from cultivated croplands in Iowa under a broad spectrum of climate variability.

The main objective of this study is to determine the extent to which projected changes in climate will impact edge-of-field surface runoff and associated sediment and nutrient losses from cultivated croplands. In particular, the specific research question is: what are the anticipated impacts of projected climate change on surface runoff and edge-of-field sediment and nutrient losses from continuous corn and corn–soybean fields in midwestern U.S. landscapes typical of northeastern Iowa? We draw attention to the differences in edge-of-field indicators between fields that receive livestock manure and those that do not, as well as between continuous corn and corn–soybean fields. We also highlight the economic implications in relation to the choice of nutrient source and availability. The results of this study contribute to our understanding of the expected trajectory of sediment and nutrient losses and will enable conservation planners and policymakers to prepare appropriate mitigation responses.

2. Materials and Methods

The fate and transport of sediment and nutrients are often simulated using a number of algorithms within ecohydrological models such as SWAT and APEX. Climate variables such as precipitation, temperature, wind speed and direction, relative humidity, and solar radiation, among others, are captured in these models to determine the impacts of weather on the growth of vegetation, soil physical and chemical characteristics, and surface runoff and leaching of nutrients. In this study, we used APEX, which has been extensively tested and validated for many locations around the world and has been specially calibrated and validated in the northeastern Iowa region that encompasses Buchanan, Fayette, Clayton, and Delaware counties [29,31]. Recent examples of APEX use in the literature include applications related to evapotranspiration [32,33], corn yields and water balance [34],

rainfall distribution and snowmelt [35], forage production [36], soybean–rice production and irrigation management [37], climate change impacts [15,21,38], phosphorus transport in subsurface tile drains [39], bacteria transport [40], rice paddy dynamics [41–43], and groundwater interactions [44]. Many other applications of APEX have been documented by Gassman et al. [27].

In a northeastern Iowa study culminating in 2000, Keith et al. [31] used the validated APEX model in conjunction with SWAT to simulate the impacts of alternative tillage practices on the yields of corn, soybeans, oats, and alfalfa in mixed livestock and crop systems in the upper Maquoketa river watershed (UMRW) in northeast Iowa, as well as water quality indicators at the outlet of the UMRW, e.g., [29]. That study also evaluated the impacts of the status quo and various conservation practices on edge-of-field runoff and nutrient and sediment losses. In the present study, we leverage the foregoing APEX validation efforts to determine the impacts of climate change on the fate and transport of edge-of-field environmental indicators on continuous corn and corn–soybean fields in Buchanan County. We use APEX because it is one of the most robust models for simulating crop growth and associated environmental implications. We also incorporate nutrient management, tillage practices, and crop yields which are representative of these earlier studies to maintain consistency with those investigations and the baseline simulation period adopted for this study (1981–2005).

The results of this study will highlight the potential impacts of climate change projections on the fate and transport of sediment and nitrogen and phosphorus from cultivated croplands. A recent study [30] used a similar methodology to project corn and soybean yields under multiple climate change scenarios.

2.1. Modeling System

APEX [25] is a comprehensive field-scale model that was initially developed in the 1990s to assess the effects of management strategies on crop growth, livestock grazing, and water quality. APEX is a modified version of the Erosion Productivity Impact Calculator (EPIC) [45] model that has been used widely to simulate alternative management scenarios such as alternative inorganic fertilizer and manure application rates, tillage practices, and the implementation of a wide array of management practices. A detailed description of APEX and how it was applied within the context of this study is provided in a recent publication [30]. For this specific application, APEX has been validated against crop yield data and water quality indicators [30]. The model is included in the Nutrient Tracking Tool (NTT) [46] and has also been calibrated and applied in numerous contexts globally [27].

2.2. Study Area

Buchanan County covers part of the western portion of the UMRW (Figure 1), which at the time of the initial APEX applications, was characterized by mixed crop and livestock production. The UMRW is a 16,200-hectare intensive livestock and crop-farming watershed in northeastern Iowa. Based on the diversity of livestock operations, manure applied on cropland represents a mix of swine, dairy, and beef cattle manures. Corn and soybean production account for about 67% of the total land area, and the watershed is characterized by extensive tile drainage. The average slope in the watershed is about 4% with a range of 1 to 16% [31]. Soils in the watershed range from fine sandy loams to clay texture, though loamy soils are predominant. In the present application, we focus solely on fields that were utilized for continuous corn or corn–soybean in 2021.

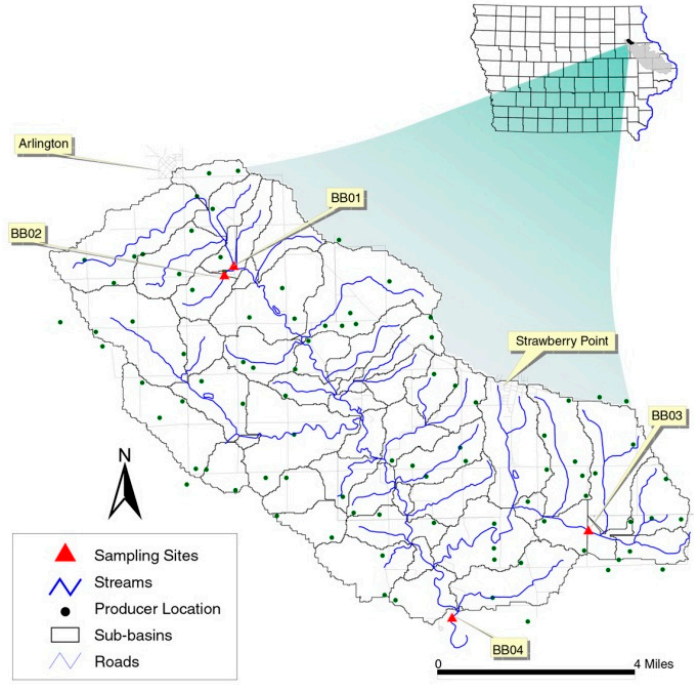

Figure 1. Upper Maquoketa River watershed at the time of initial model validations.

2.3. Data Sources

For this study, the following data were utilized. A detailed description of the data sources is provided in a recent publication [30].

2.3.1. Crop Management Data

Detailed data on field operations were obtained from producers for continuous corn and corn–soybean rotations as part of the UMRW assessments [29,31,47]. The producer information indicates that the majority utilized a reduced tillage system as their status quo crop management profile. The specific field operations used for the simulations are outlined below.

Continuous Corn Field Operations

Information on the status quo continuous corn field operations received from producers as part of the UMRW study [47] is listed in Table 1. Two types of crop nutrient management were identified based on nutrient sources: crop production with only inorganic fertilizer and crop production using a combination of inorganic fertilizer and livestock manure. Fertilizer nutrient application rates were similar between fields receiving manure versus fields that did not receive manure, with the only difference occurring for bulk spread amounts in the fall. These application rates reflect the reality of very little manure nutrient crediting by livestock producers in the UMRW as revealed in previous research [29,31]. This resulted in nitrogen fertilizer application rates that were essentially the same for fields that received manure versus fields that did not receive manure. Separate simulations were performed for fields receiving both inorganic fertilizer and manure versus those receiving only inorganic fertilizer. Using information reported by Osei et al. [47], we estimate that 15.6% of cropland areas received manure. Furthermore, it was assumed based on current data on crop distributions that 80% of corn and soybean growing areas were used for corn–soybean rotation, while only 20% was used for continuous corn. These weights—15.6% and 84.4%, respectively, for manure and non-manure field simulations and 20% and 80% for continuous corn and corn–soybean—were used to compute the weighted averages of the APEX output reported in the results section. In addition to the weighted averages, separate analyses are also presented by crop rotation and nutrient source.

Table 1. Field operations simulated for continuous corn for 1998–2000 production years.

Date	Manure Fields	Non-Manure Fields
16 April	Manure application (44.9 mt/ha)	
29 April	Herbicide application	Herbicide application
1 May	Field cultivation	Field cultivation
3 May	Regular planter	Plant
3 May	Starter fertilizer (kg/ha) (10.1 + 11.3 + 27.9)	Incorporate starter fertilizer (kg/ha) (10.1 + 11.3 + 27.9)
12 June	Row cultivate	Cultivate
18 October	Harvest corn	Harvest corn
23 October	Bulk spread (kg/ha) (17.9 + 20.2 + 41.9)	Bulk spread (kg/ha) (28.0 + 30.0 + 55.8)
2 November	Chisel plow	Chisel plow
12 November	Ammonia application (194.2 kg/ha)	Ammonia application (194.2 kg/ha)

Corn–Soybean Field Operations

Similar information was received from producers for the corn–soybean rotation, as reported in [47], reproduced in Table 2. The nutrient application rates reflect the previously described conditions indicated earlier in this section. Simulations were performed separately for fields receiving manure, as well as for fields where only inorganic fertilizer was utilized as a nutrient source. Status quo tillage practices for the corn–soybean rotation also represented a reduced tillage style of management.

Table 2. Field operations simulated for corn–soybean rotation for 1998–2000 production years.

Date	Manure Fields	Non-Manure Fields
	Corn following soybean	
16 April	Manure application (44.9 mt/ha)	
29 April	Herbicide application	Herbicide application
29 April	Fertilizer N (128.2 kg/ha)	Apply fertilizer N (128.2 kg/ha)
30 April	Field cultivation	Field cultivation
1 May	Regular planter (corn)	Regular planter (corn)
1 May	Starter fertilizer (kg/ha) (10.1 + 11.3 + 27.9)	Starter fertilizer (kg/ha) (10.1 + 11.3 + 27.9)
12 June	Cultivate	Cultivate
15 October	Harvest corn	Harvest corn
25 October	Bulk spread (kg/ha) (17.9 + 20.2 + 41.9)	Bulk spread (kg/ha) (28.0 + 30.1 + 55.8)
1 November	Chisel plow	Chisel plow
	Soybean following corn	
16 April	Manure application (44.9 mt/ha)	
29 April	Herbicide application	Herbicide application
10 May	Field cultivation	Field cultivation
12 May	Regular planter (soybean)	Regular planter (soybean)
2 October	Harvest soybean	Harvest soybean
27 October	Bulk spread (kg/ha) (15.4 + 17.3 + 41.9)	Bulk spread (kg/ha) (28.0 + 30.1 + 55.8)

For the two-year corn–soybean rotation, each polygon was divided into two equal halves, one starting in the corn year and the other starting in the soybean year, in order to ensure that each crop was simulated in each year so as to obtain an accurate weather representation for all crops. Polygon divisions were accomplished in the APEX subarea file prior to each simulation by replicating the subarea and assigning a negative sign to the second subarea, thus specifying side-by-side addition rather than routing from one half to the other.

2.3.2. Cropland Data Layer (CDL)

The GIS layer of cropland cover for Buchanan County was obtained from the USDA-NRCS data server [48]. Details of the data and how they were used for this study are provided elsewhere [30]. For continuous corn, simulations were restricted only to land

parcels that were grown in corn. Similarly, for the results associated with the corn–soybean rotation, all fields used for corn or for soybean in 2021 were simulated.

SSURGO soil data: Soil data for this study were obtained from the USDA-NRCS Soil Survey Geographic Database (SSURGO) [49]. The SSURGO data layer was overlaid on the CDL data in order to determine relevant soil types applicable to 2021 corn production fields in the study area. A total of 88,322 unique crop–soil polygons were identified as corn-growing fields for various soils within Buchanan County for 2021. Similarly, 69,651 polygons were associated with soybeans for the 2021 calendar year. Consequently, 157,973 crop–soil polygons were assigned to the corn–soybean rotation (88,322 + 69,651), while 88,322 polygons were associated with continuous corn simulations.

2.3.3. Historical Weather Data

Precipitation, minimum and maximum temperature, solar radiation, and other key weather variables were obtained from the USDA Parameter-elevation Regressions on Independent Slopes Model (PRISM) [50] database to reflect actual current and historical weather data. The PRISM weather data were used as baseline weather for the present simulations and are also available on the NTT server. The PRISM data used for this study are available at a 4 km resolution for the continental U.S. The simulations presented here were performed with a 25-year time horizon to correspond to each climate scenario's time horizon. The baseline scenario was represented by PRISM weather time series covering the 1981–2005 period since it covers the period for which APEX was calibrated and validated for the UMRW study using measured water quality data. The 1981–2005 period was also chosen because it represents the last period of historical climate data prior to the beginning of the CMIP5 projections in 2006.

2.3.4. Climate Projections

Future climate projections were obtained from the National Center for Atmospheric Research's Earth System Grid portal [51,52]. Chosen climate projections represent a middle ground, an approximate average of a best-case lower emissions scenario, and an opposite scenario wherein the current greenhouse gas emissions trajectory is maintained. Details of the climate projections are provided in Osei et al. [30] and were based on the Coupled Model Intercomparison Project—Phase 5 (CMIP5) weather projections [53,54].

Weather data on precipitation and minimum and maximum temperature were extracted from the CMIP5 databases for the following three 25-year periods for each of the future climate scenarios: 1 January 2021–31 December 2045, 1 January 2046–31 December 2070, and 1 January 2071–31 December 2095. To provide relevant context, hindcasted CMIP5 climate data were also included for two historical periods as separate climate scenarios: 1 January 1956–31 December 1980 and 1 January 1981–31 December 2005. The future climate scenarios included in this study are RCP 2.6, RCP 4.5, and RCP 8.5, which are defined according to anticipated radiative forcing levels. RCP 2.6, the most optimistic scenario of the four for reducing global warming, corresponds to a radiative forcing of 2.6 Wm^{-2} as compared to the pre-industrial era and is projected to result in a 1 °C increase in mean global temperatures by the 2046 to 2065 period. Similarly, RCP 4.5: and RCP 8.5 correspond to radiative forcing values of 4.5 Wm^{-2} and 8.5 Wm^{-2}, respectively, for the same time periods. RCP 8.5 is the most pessimistic scenario among the four for reducing global warming.

2.4. Projected Changes in Climate Patterns

The foregoing three historical and nine projected climate outcomes—twelve in all—were simulated in this study. Other than the PRISM scenario, the two historical and nine projected CMIP5 scenarios are global climate model projections and are consequently not actual climate realizations. Additional information and analysis related to climate projections are provided elsewhere [30]. Each climate scenario presents a unique pattern of weather trajectory for Buchanan County and is summarized in this section as averages

across all grid points included in the simulations. However, simulations were based on data for individual grid points.

2.5. Climate Scenarios Simulated

A summary of the climate scenarios is provided in Table 3. A total of twelve climate scenarios were simulated: the baseline (PRISM for 1981–2005), two hindcasted CMIP5 scenarios, and nine CMIP5 climate projections—three time periods each for RCP2.6, RCP4.5, and RCP8.5. In some of the analyses below, we will also use the 1981–2005 hindcasted CMIP5 scenario as an alternative baseline to which the twelve CMIP5 scenarios will be compared.

Table 3. Specific Climate Scenarios included in this study.

Scenarios	1956–1980	1981–2005	2021–2045	2046–2070	2071–2095
Historical (CMIP5)	X	X *	-	-	-
Historical (PRISM)		X: Baseline			
RCP 2.6 (CMIP5)		-	X	X	X
RCP 4.5 (CMIP5)		-	X	X	X
RCP 8.5 (CMIP5)		-	X	X	X

* Used as alternative baseline, a CMIP5 baseline for comparing outcomes of CMIP5 projections.

Projected climate patterns are clearly different from current realizations. Average annual precipitation—averages taken over each 25-year time horizon—are shown in Table 4, and virtually all precipitation values shown in the table are significantly different from each other at a 5% level of significance. Annual precipitation levels are clearly projected to increase with all CMIP5 climate projections as compared to hindcasted values. However, the actual gridded (PRISM) precipitation for the "current" (1981–2005) historical time period is also significantly higher than the hindcasted CMIP5 values for the same time period. For all projections, RCP8.5 promises the greatest increase in annual precipitation totals, with the highest in the 2021–2045 period.

Table 4. Annual precipitation by climate scenario: mean, minimum, and maximum (mm/year).

Scenario	1956–1980	1981–2005	2021–2045	2046–2070	2071–2095
Historical (CMIP5)	882 (616, 1149)	874 (669, 1039)			
Historical (PRISM)		886 (535, 1222)			
RCP 2.6 (CMIP5)			876 (444, 1231)	907 (614, 1228)	904 (543, 1298)
RCP 4.5 (CMIP5)			860 (615, 1094)	914 (575, 1231)	907 (661, 1166)
RCP 8.5 (CMIP5)			973 (588, 1367)	950 (639, 1165)	967 (696, 1291)

The numbers in Table 4 are, respectively, the average annual precipitation, followed by the minimum and maximum annual precipitation values in parentheses, each averaged across all grid points simulated. The future CMIP5 annual precipitation projections are clearly indicated to have a broader range than the hindcasted values, particularly in the case of RCP 2.6.

To better highlight the trends and variability in annual precipitation levels, Figure 2 shows the trends in average annual precipitation, each line graph covering the entire 75-year time series of future CMIP5 projections and the 50-year time period of hindcasted (historical) CMIP5 data. For simplicity of exposition, the figure excludes the PRISM series. The legends displayed in the figure also show, respectively, in parentheses, the mean and standard error of each CMIP5 series. As often stated in the literature, RCP 8.5 is projected to result in wetter conditions. All CMIP5 projections indicate a greater variability of annual precipitation patterns, with RCP 2.6 associated with the highest standard error. Analyses of these climate projection data are relevant because they are the underpinnings of future

trends in surface runoff and associated sediment and nutrient losses. Various studies similarly analyze these patterns to better elucidate the output from model simulations, e.g., [15,21,38].

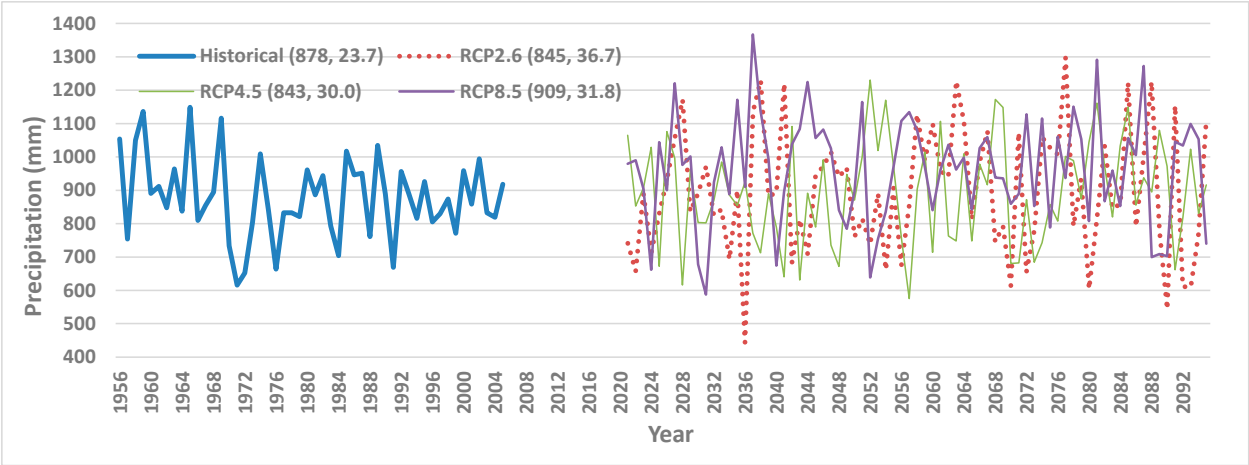

Figure 2. Trends in average annual precipitation by CMIP5 climate scenario.

Besides being the wettest climate projection, RCP 8.5 is also associated with the highest average temperatures. Both average monthly minimum temperatures and average monthly maximum temperatures are highest with RCP 8.5. RCP 8.5 is associated with the highest minimum and maximum temperatures, as expected, particularly for the 2071–2095 period as compared to other CMIP5 projections. This is particularly true of the June through September months, where RCP 8.5 monthly maximum temperatures are markedly higher than those of the other two RCP projections. These and additional analyses of projected temperature and precipitation patterns are provided by Osei et al. [30].

Higher temperatures and precipitation levels with RCP 8.5 mean that growing conditions will be warmer and wetter. While not shown here, precipitation levels under all CMIP5 scenarios—particularly RCP 8.5—are expected to favor high-intensity storm events, which implies that a greater portion of total precipitation volumes for the year are associated with a few major storms. As reported in previous studies [16,55], these precipitation outcomes indicate a greater likelihood of surface runoff losses even if total precipitation volumes are the same. Monthly precipitation averages also suggest that a major portion of annual precipitation increases associated with RCP 8.5 for the 2021–2045 period will likely occur in the August through November period, partly but not wholly, benefiting corn and soybean crops close to grain maturity for harvesting.

2.6. APEX Validation

As mentioned above, APEX was calibrated and validated for agronomic and edge-of-field environmental indicators as part of the UMRW study [31]. Subsequently, Osei et al. [30] completed further validation tests to show that the model performs very well in simulating surface runoff and sediment losses. Nitrogen and phosphorus losses in surface runoff are also quite close to validated results from the UMRW study, as shown here in Table 5. Thus, we consider APEX sufficiently validated for the current study. The values of key APEX parameters that were determined from the validation process are reported in Osei et al. [30].

Table 5. APEX model validation results for 1998–2000 application in northeast Iowa.

Agronomic or Environmental Indicator	Measured Data		Simulated
	Value	Source and Notes	Value
Crop yields (mt/ha): 1997–1999 production years			
Continuous corn yield (mt/ha)	8.34	Average from UMRW	8.30
Corn following soybean yield (mt/ha)	8.60	study [47]. Obtained from	8.31
Soybean yield (mt/ha)	3.22	survey of producers.	3.54
Surface runoff (mm)			
From USEPA [56]: data by HUC *	88.3	Buchanan County: 2002	79.3
From Osei et al. [47]	65.1	Flow for UMRW	79.3
Sediment loss from fields (mt/ha)			
From USEPA [56]: data by HUC *	1.66	Buchanan County: 2002	2.71
From Osei et al. [47]	2.24	Sediment loss from UMRW	2.71
N loss in surface runoff from fields (kg/ha)			
From Osei et al. [47]	6.11	Buchanan County: 2002	2.70
Sediment-bound N loss from fields (kg/ha)			
From Osei et al. [47]	16.7	Buchanan County: 2002	16.44
P loss in surface runoff from fields (kg/ha)			
From Osei et al. [47]	0.64	Buchanan County: 2002	0.70
Sediment-bound P loss from fields (kg/ha)			
From Osei et al. [47]	3.36	Buchanan County: 2002	1.61

* Measured data represent averages for 2002 for all hydrologic unit codes (HUCs) in Buchanan County, Iowa.

2.7. Simulation Procedure

APEX simulation results reported by Osei et al. [30] indicated that results from 20% of randomly selected crop–soil polygons are practically the same as (statistically indistinguishable from) results based on 100% of the population of crop–soil polygons for continuous corn and corn–soybean in Buchanan County. Consequently, for this study, 20% of randomly selected crop–soil polygons were simulated for each rotation. This represents 17,664 polygons for continuous corn and 31,595 polygons for the corn–soybean rotation. Additional details of the simulation procedure are provided in [30].

3. Results and Discussion

The environmental indicators of interest in this study are the following edge-of-field indicators: surface runoff, sediment losses, and the totals and key components of nitrogen and phosphorus losses. To obtain the results reported here, output from all crop–soil polygons simulated were merged in SAS®, which was used to compute an area-weighted average and other summary statistics for each indicator and for each scenario. We first present weighted average impacts across both crop rotations and averaged also across fields receiving manure and those receiving only inorganic fertilizer.

3.1. Average Climate Change Impacts across All Crop Rotations and Nutrient Sources

Summary results are arranged by indicator, by major climate scenario, and by time period in Tables 6–8. The results for surface runoff and sediment losses are shown in Table 6, Total Nitrogen and its key components in Table 7, and Total Phosphorus and its key components in Table 8. In each table, we display results by major climate scenario in rows and time periods in columns going from left to right in chronological order. In Tables 6–8, average annual values for each respective indicator are reported, followed in parentheses by two percentage change values. The first percentage change is relative to the baseline scenario, the 1981–2005 PRISM climate scenario. The second percentage change is relative to the 1981–2005 historical CMIP5 value, which served as an alternate baseline for CMIP5 comparisons. The reason for the two percentage changes will become apparent later on.

Table 6. Simulated impacts of climate scenarios on average annual edge-of-field surface runoff and sediment losses based on 1998–2000 management practices.

Scenario	1956–1980	1981–2005	2021–2045	2046–2070	2071–2095
Average annual surface runoff: mm (% changes from PRISM and CMIP5 baselines *)					
Historical (CMIP5)	85.6 (−36, 16)	73.7 (−45, 0)			
Historical (PRISM)		133.4 (0, 81)			
RCP 2.6 (CMIP5)			105.8 (−21, 44)	90.9 (−32, 23)	97.5 (−27, 32)
RCP 4.5 (CMIP5)			91.3 (−32, 24)	114.8 (−14, 56)	95.8 (−28, 30)
RCP 8.5 (CMIP5)			132.8 (0, 80)	116.5 (−13, 58)	118.7 (−11, 61)
Average annual sediment losses: mt/ha (% changes from PRISM and CMIP5 baselines *)					
Historical (CMIP5)	0.8 (−62, 13)	0.7 (−66, 0)			
Historical (PRISM)		2.0 (0, 198)			
RCP 2.6 (CMIP5)			1.7 (−16, 150)	1.3 (−32, 102)	1.5 (−23, 131)
RCP 4.5 (CMIP5)			1.7 (−15, 152)	2.0 (−1, 197)	1.4 (−31, 106)
RCP 8.5 (CMIP5)			1.5 (−27, 119)	2.0 (1, 201)	3.0 (48, 343)

* Numbers in parentheses are respective percentage changes from the 1981–2005 PRISM baseline and 1981–2005 historical (hindcasted) CMIP5 values.

Table 7. Simulated impacts of climate scenarios on average annual edge-of-field nitrogen losses based on 1998–2000 management practices.

Scenario	1956–1980	1981–2005	2021–2045	2046–2070	2071–2095
Average annual soluble N losses: kg/ha (% changes from PRISM and CMIP5 baselines *)					
Historical (CMIP5)	3.6 (−31, 7)	3.4 (−36, 0)			
Historical (PRISM)		5.3 (0, 55)			
RCP 2.6 (CMIP5)			4.5 (−14, 33)	5.0 (−5, 47)	4.3 (−19, 26)
RCP 4.5 (CMIP5)			5.0 (−5, 47)	7.4 (40, 118)	5.1 (−3, 51)
RCP 8.5 (CMIP5)			7.0 (32, 105)	6.0 (14, 77)	8.4 (60, 147)
Average annual sediment-bound N losses: kg/ha (% changes from PRISM and CMIP5 baselines *)					
Historical (CMIP5)	8.4 (−55, 12)	7.5 (−60, 0)			
Historical (PRISM)		18.7 (0, 150)			
RCP 2.6 (CMIP5)			14.4 (−23, 92)	11.6 (−38, 55)	12.6 (−33, 68)
RCP 4.5 (CMIP5)			13.1 (−30, 75)	16.1 (−14, 115)	12.5 (−33, 67)
RCP 8.5 (CMIP5)			14.3 (−23, 91)	15.9 (−15, 112)	20.3 (8, 171)
Average annual total N losses: kg/ha (% changes from PRISM and CMIP5 baselines *)					
Historical (CMIP5)	12.0 (−50, 10)	10.9 (−55, 0)			
Historical (PRISM)		24.0 (0, 120)			
RCP 2.6 (CMIP5)			18.9 (−21, 73)	16.6 (−31, 52)	16.9 (−30, 55)
RCP 4.5 (CMIP5)			18.1 (−25, 66)	23.4 (−2, 116)	17.6 (−27, 62)
RCP 8.5 (CMIP5)			21.3 (−11, 96)	21.9 (−9, 101)	28.7 (20, 164)

* Numbers in parentheses are respective percentage changes from the 1981–2005 PRISM baseline and 1981–2005 historical (hindcasted) CMIP5 values.

The top section of Table 6 presents the APEX simulation results for surface runoff. The table indicates that average surface runoff from corn and soybean fields would vary widely depending on the climate scenario. The highest average annual runoff volume—133.4 mm/year—is associated with the PRISM baseline, followed closely by the 2021–2045 period of RCP 8.5. The other ten climate scenarios are associated with markedly lower surface runoff volumes. Thus, percentage changes in surface runoff volumes from the PRISM baseline are all negative or practically zero.

Table 8. Simulated impacts of climate scenarios on average annual edge-of-field phosphorus losses based on 1998–2000 management practices.

Scenario	1956–1980	1981–2005	2021–2045	2046–2070	2071–2095
Average annual soluble P losses: kg/ha (% changes from PRISM and CMIP5 baselines *)					
Historical (CMIP5)	0.6 (−37, 11)	0.5 (−44, 0)			
Historical (PRISM)		1.0 (0, 78)			
RCP 2.6 (CMIP5)			0.8 (−15, 52)	0.7 (−29, 26)	0.7 (−24, 35)
RCP 4.5 (CMIP5)			0.7 (−31, 23)	0.9 (−7, 65)	0.8 (−20, 42)
RCP 8.5 (CMIP5)			1.0 (7, 90)	0.9 (−8, 64)	0.9 (−5, 69)
Average annual sediment-bound P losses: kg/ha (% changes from PRISM and CMIP5 baselines *)					
Historical (CMIP5)	0.8 (−60, 8)	0.7 (−63, 0)			
Historical (PRISM)		1.9 (0, 169)			
RCP 2.6 (CMIP5)			1.5 (−21, 113)	1.3 (−33, 80)	1.4 (−29, 92)
RCP 4.5 (CMIP5)			1.5 (−20, 116)	1.8 (−8, 148)	1.3 (−31, 86)
RCP 8.5 (CMIP5)			1.5 (−20, 116)	1.8 (−7, 150)	2.5 (32, 256)
Average annual total P losses: kg/ha (% changes from PRISM and CMIP5 baselines *)					
Historical (CMIP5)	1.4 (−52, 9)	1.3 (−56, 0)			
Historical (PRISM)		2.9 (0, 129)			
RCP 2.6 (CMIP5)			2.3 (−19, 87)	2.0 (−32, 56)	2.1 (−27, 67)
RCP 4.5 (CMIP5)			2.2 (−23, 76)	2.7 (−8, 112)	2.1 (−27, 67)
RCP 8.5 (CMIP5)			2.6 (−11, 105)	2.7 (−7, 113)	3.4 (20, 174)

* Numbers in parentheses are respective percentage changes from the 1981–2005 PRISM baseline and 1981–2005 historical (hindcasted) CMIP5 values.

However, it is important to note what the hindcasted climate scenarios imply. They represent the historical climate regime that is implied by the CMIP5 climate projections. In other words, the processes that generated the CMIP5 projections for 2021–2045, 2046–2070, and 2071–2095 imply a historical climate record that is mimicked by the CMIP5 historical data series in the 1956–1980 and 1981–2005 time periods. This means that in addition to the comparison to the PRISM baseline, we should also compare the projected indicators to the corresponding values of the CMIP5 historical scenario, particularly for the 1981–2005 period that we consider as the baseline time period.

Comparison of surface runoff volumes for each scenario to that of the 1981–2005 historical CMIP5 surface runoff leads to the expectation that surface runoff volumes will be much higher than current levels if the historical CMIP5 conditions adequately represent current conditions. The percentage changes indicate that ignoring the PRISM baseline, the highest increases in surface runoff volumes will be associated with RCP 8.5, particularly the 2021–2045 period, when we should expect an 80% increase in surface runoff compared to the historical CMIP5 levels in the 1981–2005 period. Admittedly, anthropogenic effects such as human activities related to cropland management have an impact on surface runoff losses. However, as we will see in the next section, these losses are overwhelmingly driven by climate patterns, primarily storm events.

It is insightful to note that annual average surface runoff is significantly correlated with annual average precipitation (see Table 9). However, the weighted average aggregates presented in Table 6 do not necessarily correspond to the relative precipitation levels presented in Table 4. This is because, as expected, average annual aggregates even out variabilities inherent in daily patterns that are, in reality, the drivers of surface runoff volumes and other environmental indicators. Average annual aggregates are two steps away from daily precipitation and runoff events, as they are first annual aggregates, and then secondly, averages of the annual aggregates across the crop-soil polygons simulated. For this reason, while average annual precipitation is much higher in the 2021–2045 period of RCP 8.5 than the PRISM baseline, average annual surface runoff volumes are roughly the same between the two scenarios.

Table 9. Correlation coefficients between selected average annual indicators *.

Indicator	Precipitation	Surface Runoff	Sediment	Sediment-Bound N	Soluble N	Sediment-Bound P	Soluble P
				Correlation matrix for hindcasted CMIP5 series			
Precipitation	1.00	0.64	0.47	0.49	0.56	0.49	0.50
Surface runoff	0.64	1.00	0.50	0.54	0.70	0.53	0.85
Sediment loss	0.47	0.50	1.00	0.98	0.55	0.96	0.07
				Correlation matrix for CMIP5 RCP 2.6 series			
Precipitation	1.00	0.74	0.60	0.65	0.61	0.65	0.67
Surface runoff	0.74	1.00	0.72	0.76	0.60	0.75	0.93
Sediment loss	0.60	0.72	1.00	0.99	0.39	0.98	0.51
				Correlation matrix for CMIP5 RCP 4.5 series			
Precipitation	1.00	0.71	0.57	0.60	0.52	0.60	0.66
Surface runoff	0.71	1.00	0.71	0.76	0.66	0.74	0.95
Sediment loss	0.57	0.71	1.00	0.99	0.52	0.98	0.54
				Correlation matrix for CMIP5 RCP 8.5 series			
Precipitation	1.00	0.80	0.63	0.67	0.59	0.64	0.74
Surface runoff	0.80	1.00	0.70	0.74	0.60	0.70	0.94
Sediment loss	0.63	0.70	1.00	0.99	0.45	0.98	0.56

* Each row shows correlation coefficients between variable named in the row and variables in column header. All indicators were computed as weighted averages across all crop–soil polygons simulated. All correlation coefficients are highly significant except for correlation between sediment loss and soluble P under hindcasted CMIP5 series.

Similar comparisons can be made among other climate scenarios. Nonetheless, broad comparisons to hindcasted CMIP5 baseline data indicate that a significant increase in surface runoff is in store, particularly if RCP 8.5 materializes.

The lower portion of Table 6 presents results for sediment losses in mt/ha/year. Once again, the losses during the PRISM baseline are among the highest, except for the 2046–2070 and 2071–2095 periods of RCP 8.5. However, comparisons to the hindcasted CMIP5 results suggest that sediment losses may likely increase dramatically even under RCP 2.6 and RCP 4.5. Compared to the hindcasted CMIP5 results for 1981–2005, sediment losses would more than double for all projected climate scenarios (a percentage change greater than 100) and could triple (a percentage change of 200) in the 2046–2070 period of RCP 4.5 or RCP 8.5, or even more than quadruple (a percentage change greater than 300) in the 2071–2095 period of RCP 8.5. The hindcasted CMIP5 data suggest that these dramatic increases in sediment losses are all possible relative to the 1981–2005 period, if, again, the CMIP5 baseline represents current reality as compared to future climate patterns. Once again, it is not possible to infer these dramatic increases just by a comparison of average annual input and output indicators. The correlations shown in Table 9, though highly significant in most cases, do not reflect the underlying daily variations. It is partly for these reasons that econometric models based on aggregates often fail to adequately predict environmental indicators from widely available aggregate data.

Surface runoff and sediment losses are the two main conduits for edge-of-field nutrient losses from cropland. Soluble nutrients such as nitrates and phosphates are transported as dissolved minerals in runoff water. Similarly, sediment-bound nutrients such as sediment-bound nitrogen and phosphorus (mostly as organic compounds) are transported attached to sediment particles that leave the fields in surface runoff. The results in Tables 7 and 8 show both soluble and sediment-bound nutrient losses from cropland as well as corresponding total nitrogen and total phosphorus losses in kg/ha/year.

The top section of Table 7 shows soluble nitrogen losses followed by sediment-bound nitrogen in the middle section and total nitrogen at the bottom section of the table. In the case of soluble nitrogen losses, the hindcasted CMIP5 results are not as drastically different from the PRISM baseline as is the case with other indicators we present in this study. Consequently, regardless of which reference point we use, most of the CMIP5 projections

call for a significant increase in soluble nitrogen losses as compared to the PRISM baseline or hindcasted CMIP5 results. For the most part, soluble N losses are projected to more than double under RCP 8.5 as compared to hindcasted CMIP5 results. This corresponds well with various published studies [57,58] that also project substantially increased nitrate losses as a result of climate change. Soluble N loss increases are considerably smaller in magnitude under RCP 4.5 and especially RCP 2.6 as compared to RCP 8.5.

Sediment-bound nitrogen losses are projected to follow a pattern similar to sediment losses. CMIP5 projections are mostly lower than under the PRISM baseline. However, comparisons to hindcasted CMIP5 results in 1981–2005 suggest dramatic increases for most climate scenarios if the CMIP5 baseline is a good reference point. Due to the fact that sediment-bound N losses are much larger in magnitude than soluble N losses, for the most part, total N losses follow the pattern of sediment-bound N losses.

A corresponding set of results is provided in Table 8 for phosphorus, with soluble P, sediment-bound P, and total P, respectively, in the top, middle, and bottom sections of the table. Once again, with few exceptions, the PRISM baseline is associated with the highest losses. Soluble P losses are highest with the 2021–2045 period of RCP 8.5 at 1.0 kg/ha/year, roughly the same as with the PRISM baseline. However, when compared to hindcasted CMIP5 results, all climate scenarios are projected to result in increased edge-of-field soluble P losses, with the highest associated with RCP 8.5.

The pattern of results is similar for sediment-bound P losses, with the 2071–2095 period of RCP 8.5 registering the highest losses, at 2.5 kg/ha/year, followed by the PRISM baseline at 1.9 kg/ha/year. When compared to hindcasted CMIP5 values, all climate change projections are once again anticipated to result in dramatic increases in edge-of-field losses of sediment-bound P, as much as a 256% increase in the 2071–2095 period of RCP 8.5. Finally, since sediment-bound P losses are greater in magnitude than soluble P losses, total P losses mirror the patterns of sediment-bound P losses.

The climate change impacts shown in Tables 6–8 highlight the relative values of average edge-of-field surface runoff and sediment and nutrient losses. However, one important aspect of climate change impacts—variability inherent in the year-to-year runoff and sediment and nutrient losses—is not reflected in these tables. To highlight the trends and variability of these indicators, we present their time trends in charts. The charts are displayed by a major CMIP5 climate scenario: 50 years of combined data for the historical CMIP5 scenarios (1956–2005) and 75 years of combined time series (2021–2095) for each of the CMIP5 RCP scenarios (RCP 2.6, RCP 4.5, and RCP 8.5). Each of the charts also displays the overall mean and standard error of the major time series as part of the legend.

The trends of surface runoff (Figure 3) indicate that not only are the levels of surface runoff losses expected to increase for each climate change projection as compared to the CMIP5 baseline, as already shown in Table 6, but they also become more variable. Average surface runoff levels for a given year—averaged across all crop-soil polygons—can be as high as 350 mm and as low as well below 50 mm for RCP 8.5. Similar variabilities are displayed for RCP 2.6 and RCP 4.5, though not as pronounced. In contrast, the maximum average annual surface runoff for a given year—averaged across all simulated crop–soil polygons—was only as high as about 200 mm under historical CMIP5 conditions.

Similar comparisons are obtained for trends in average annual sediment losses in the runoff for the CMIP5 scenarios (Figure 4). Other than being associated with higher sediment losses compared to hindcasted CMIP5 conditions, the year-to-year variability in sediment losses is very pronounced under the CMIP5 projections, particularly under RCP 8.5 and RCP 2.6, where average annual sediment losses can be as high as 8 mt/ha—an average across all crop–soil polygons simulated—compared to an average peak of barely 5 mt/ha/year under hindcasted CMP5 conditions. Furthermore, while the variability in sediment losses under hindcasted CMIP5 conditions appears to be attenuated over time, that is not the case with RCP 2.6, RCP 4.5, and RCP 8.5 projections, with variabilities maintained throughout the time series. Means and standard errors for sediment losses under each CMIP5 projection are considerably higher than for the hindcasted series.

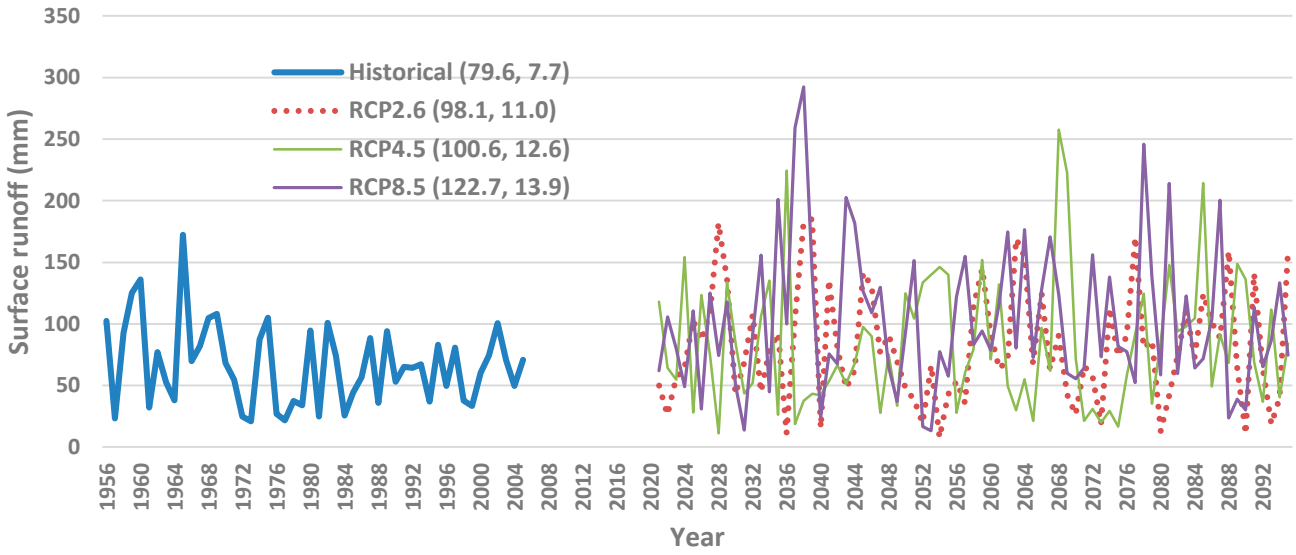

Figure 3. Trends in average annual surface runoff by CMIP5 climate scenario.

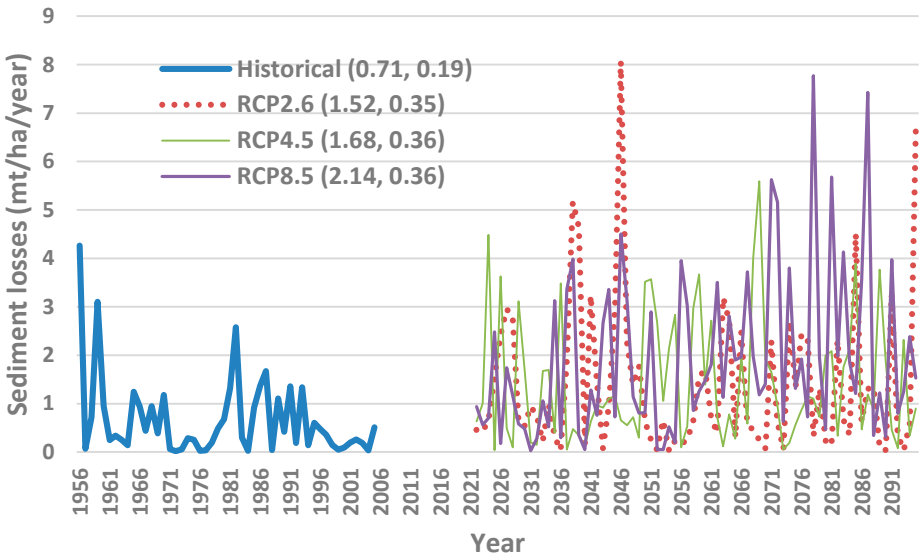

Figure 4. Trends in average annual sediment losses in runoff by CMIP5 climate scenario.

Trends for key components of nitrogen and phosphorus losses are shown in Figure 5. As with the case for surface runoff and sediment losses, the figure shows without exception that there will be increased variability of soluble and sediment-bound components of nitrogen and phosphorus as compared to hindcasted CMIP5 conditions. In each case, means and standard errors are higher with all three CMIP5 projections than the hindcasted CMIP5 series. Among the three CMIP5 projections, means and standard errors of soluble and sediment-bound nitrogen and phosphorus are consistently the highest with RCP 8.5 and lowest with RCP 2.6.

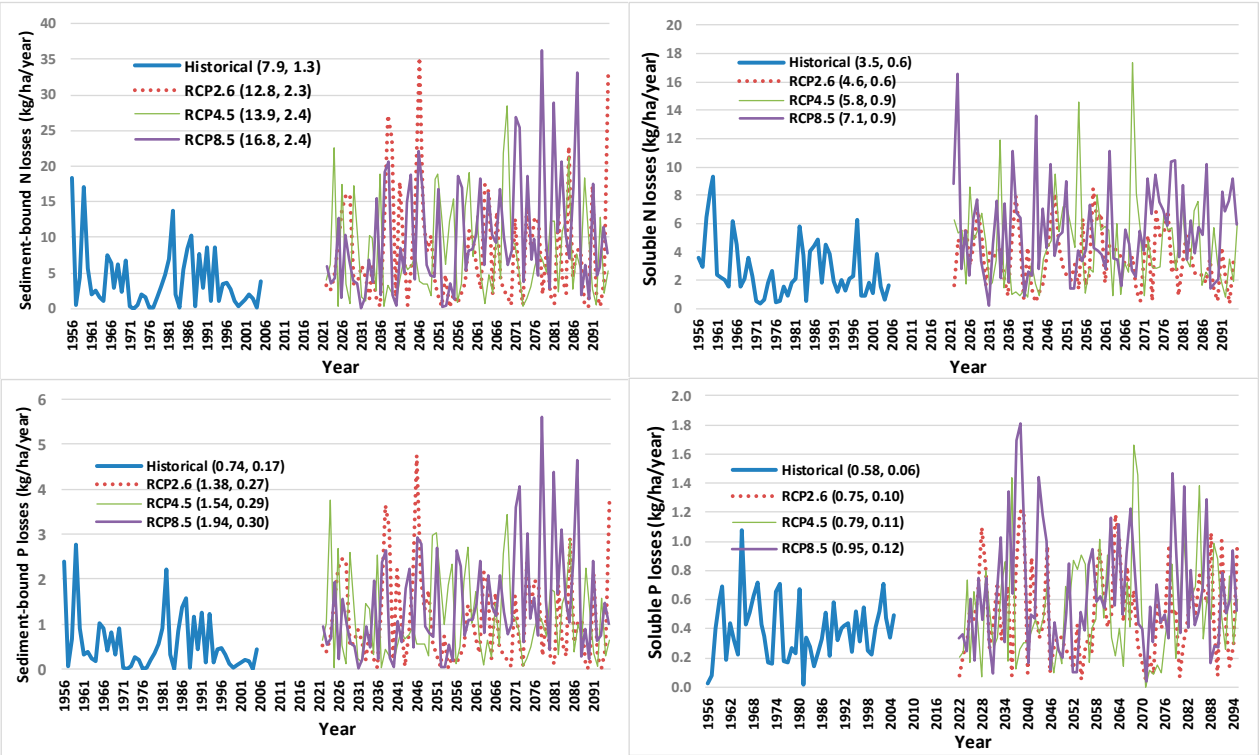

Figure 5. Trends in annual nutrient losses in runoff by CMIP5 climate scenario.

3.2. Climate Change Impacts by Crop Rotation and Nutrient Source

The edge-of-field results presented thus far have been weighted averages across all crop–soil polygons of a given crop and then averaged across both continuous corn and corn–soybean rotations both for fields using manure and those utilizing only inorganic fertilizers. We now turn to the climate change impacts for specific crop and nutrient source combinations. In particular, we explore results for continuous corn fields receiving manure (M) and fields that do not receive manure (N-M). Similarly, we analyze results from corn–soybean fields receiving manure (M) and those not receiving manure (N-M). In the following tables of results, the names of all climate scenarios are listed in the first column and the results for various indicators are presented by rotation and type of nutrient source in separate columns from left to right.

The first set of results is presented in Figure 6 for surface runoff and sediment losses. A fairly consistent but distinct set of impacts are revealed for both surface runoff and sediment losses. Surface runoff losses are quite similar regardless of rotation or nutrient source. However, there is a slight elevation of surface runoff when continuous corn is planted rather than a corn–soybean rotation. This underscores the fact that climate differences have a much greater direct impact on surface runoff losses than differences in cropland management or other human activities. In other words, differences in surface runoff losses for a given climate regime, but with different land management practices or other human activities, are dwarfed by differences in surface runoff losses for a given management practice but different climate regimes.

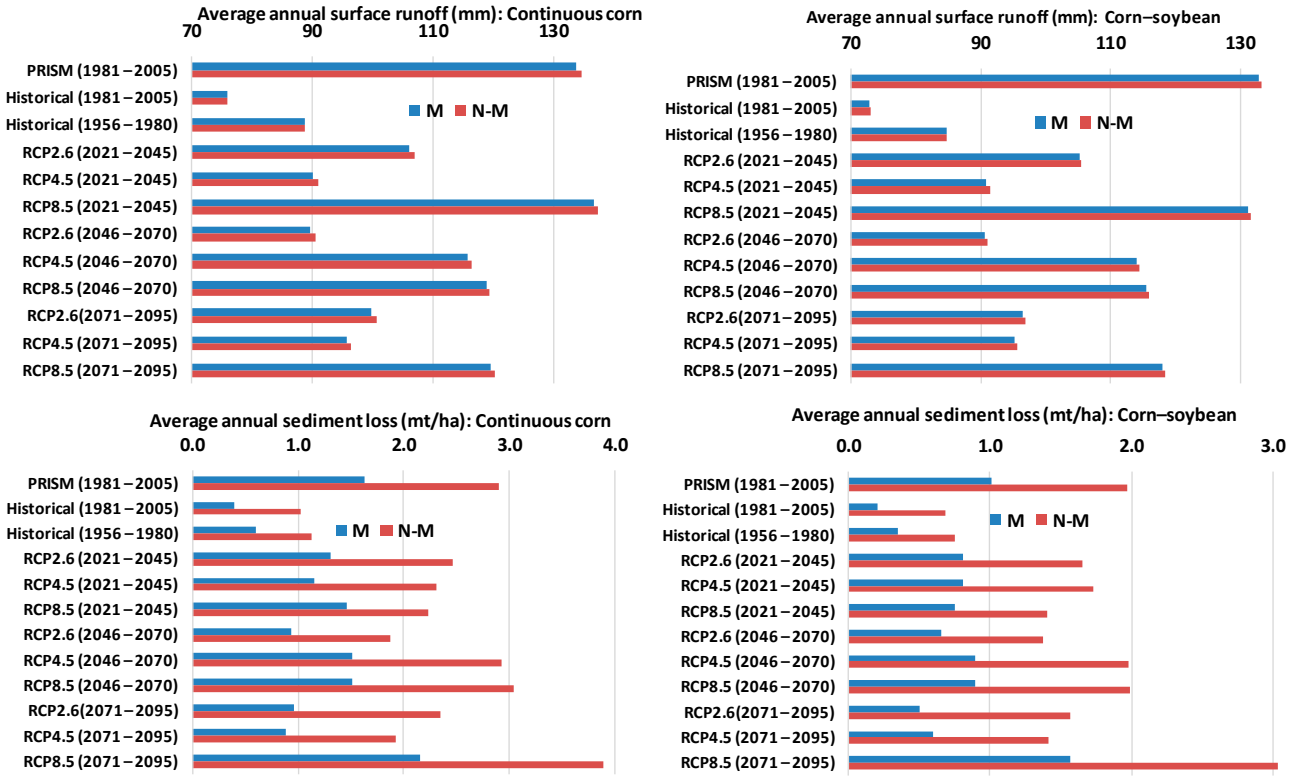

Figure 6. Edge-of-field surface runoff and sediment losses by rotation and nutrient source.

On the other hand, there are clear distinctions regarding sediment losses. Average annual sediment losses are higher for continuous corn than for the corn–soybean rotation. This may be due primarily to the fact that there are very minimal tillage operations on soybeans as compared to corn in this area. Furthermore, sediment losses are also higher for fields that do not receive manure. Specifically, sediment losses on fields not receiving manure are roughly double the rate associated with fields that receive manure. This result is explained by the fact that the increased organic matter associated with manure applications serves to reduce erosion rates.

Edge-of-field soluble N and sediment-bound N results are presented in Figure 7, also with crop rotation and nutrient source for each climate scenario. The results are markedly different by rotation and by nutrient source. Soluble N losses are clearly higher from manure fields than from fields not receiving manure. Since surface runoff losses are roughly similar for all rotations and nutrient sources, it implies that surface runoff losses from fields receiving manure have a higher concentration of soluble N than from fields that do not receive manure. Thus, this result may be largely predicated upon the manure application rate versus the rate of nutrient application on fields not receiving manure; total nutrient application rates are clearly higher on fields receiving manure. Finally, soluble N losses are also higher from continuous corn fields than from corn–soybean fields.

The differences in results presented in Figure 7 for sediment-bound N losses are even more marked between rotation and between nutrient sources. Depending on the climate scenario, sediment-bound N losses from fields receiving manure are roughly quadruple those from fields that do not receive manure. Similarly, sediment-bound N losses are consistently higher from continuous corn fields than from corn–soybean fields. Since sediment losses were shown to be higher with continuous corn fields, it is clear that a portion of the increased sediment-bound N loss associated with the continuous corn rotation is due to increased sediment losses. However, sediment losses were shown to be lower with fields receiving manure. Thus, the fact that sediment-bound N losses are higher with manure fields implies a drastically higher concentration of sediment-bound N that

more than offsets the lower rate of sediment losses from fields receiving manure. Once again, management practices, in particular, nutrient application rates, may hold the key to reduced nutrient losses in this case. Changes in inorganic fertilizer prices may impact producer nutrient utilization practices, and in turn impact nutrient losses, as also reported by Xu et al. [1].

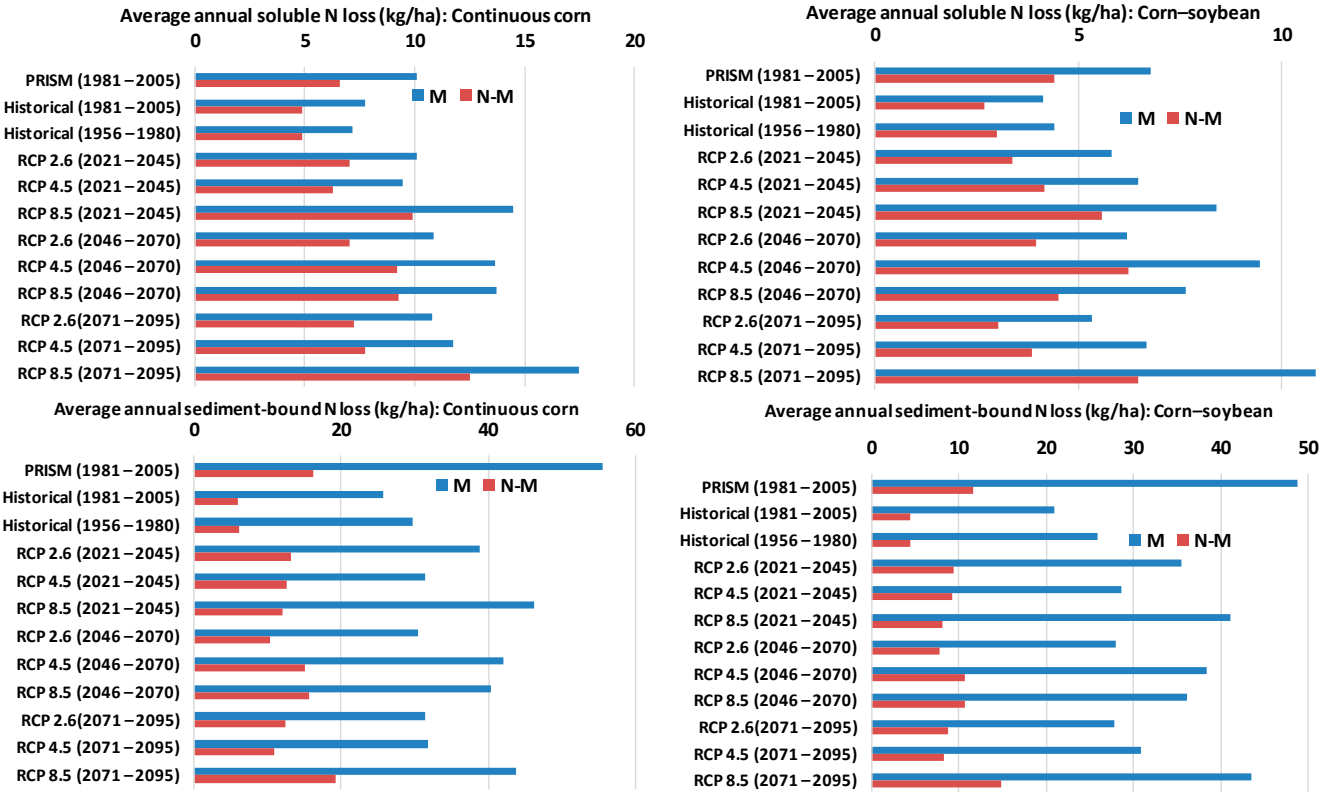

Figure 7. Edge-of-field soluble and sediment-bound N losses by rotation and nutrient source.

The final set of results is shown in Figure 8 for soluble P and sediment-bound P losses. Once again, the results are quite consistent, though not in all cases. The results for soluble P losses are consistent: soluble P losses are higher from corn fields, and at least double from fields receiving manure as compared to fields not receiving manure. The results for sediment-bound P are less consistent. Sediment-bound P losses are mostly higher from continuous corn fields than corn–soybean fields, but not always. Similarly, they are mostly higher from fields receiving manure than from fields not receiving manure, again with few exceptions.

The disparity of the results between crop rotations and nutrient sources highlights some important economic implications. If producers choose to switch more fields from corn–soybean to continuous corn due to market conditions, nutrient losses may be exacerbated. Similarly, on fields where manure is applied, we may see higher nutrient losses even if erosion rates are lower. It may be useful to determine to what extent this result is due to the manure application rate. It is clear that as inorganic fertilizer prices rise, more use will be made of livestock manure, raising the importance of the role of fields receiving manure in the overall management of edge-of-field nutrient losses to downstream waters.

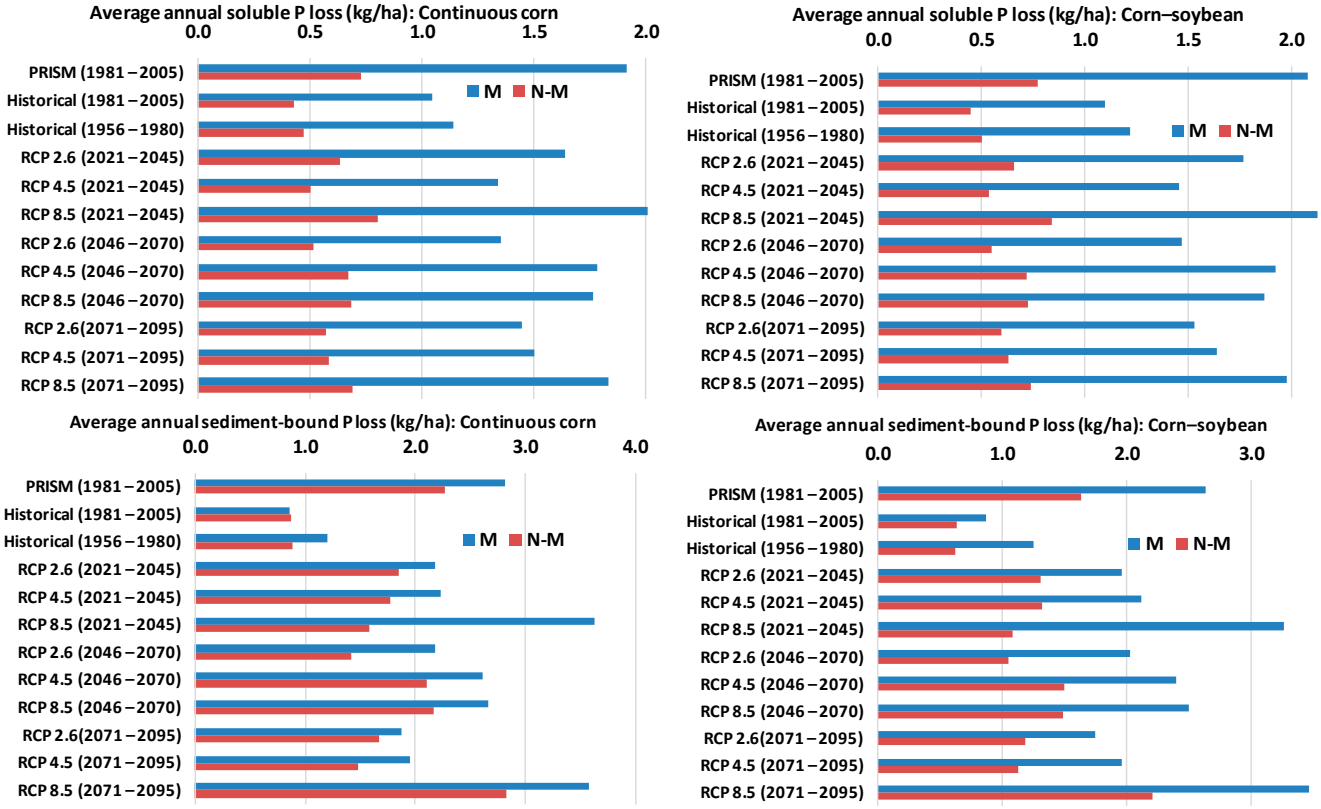

Figure 8. Edge-of-field soluble and sediment-bound P losses by rotation and nutrient source.

4. Conclusions

Well-documented scientific studies indicate long-term atmospheric warming trends over the past 100 years in the U.S., providing supporting evidence of global climate change. If forecasted changes in climate materialize, there will be impacts on agricultural land areas and relative ecological implications that are yet to be well understood. In this study, we contribute to the general understanding of these impacts by projecting the impacts of various climate change scenarios on surface runoff and sediment and nutrient losses from croplands in Buchanan County, Iowa, a county in the heart of the U.S. Corn Belt where corn and soybean productions are predominant land uses.

To determine the impacts of climate change on the aforementioned ecological indictors, twelve climate scenarios were specified. Nine future CMIP5 climate change projections consisted of three climate change model scenarios—RCP 2.6, RCP 4.5, and RCP 8.5—each evaluated over three 25-year time periods: 2021–2045, 2046–2070, and 2071–2095. Two hindcasted CMIP5 climate scenarios for two 25-year time periods—1956–1980 and 1981–2005—were also included, which gauge what the climate would have been in the past if the future CMIP5 outcomes are plausible. Finally, the twelfth climate scenario is the actual, albeit gridded, "current" realization: the PRISM time series for the 1981–2005 period, which served as the main baseline. The hindcasted CMIP5 scenario for 1981–2005 was also used as an alternate baseline for various comparisons.

Climate scenarios were simulated for continuous corn and corn–soybean fields. To this end, the SSURGO soils database was overlaid on the CDL crop layer for 2021 to determine appropriate crop–soil polygons to simulate. The closest climate grid point for each polygon was determined by proximity based on the minimum Euclidean distance between the grid point and centroid of the crop–soil polygon. A random selection of 20% of polygons was then simulated in APEX, an ecohydrological model that was calibrated and validated for such use in northeastern Iowa.

Results of the scenario simulations indicate that, depending on the reference point of comparison, surface runoff and sediment and nutrient losses are likely to increase substantially under future climate change regimes. However, regardless of the point of reference, and regardless of which climate scenario materializes, soluble N losses are projected to increase substantially. If the point of reference is the hindcasted CMIP5 baseline, all ecological indicators will increase substantially.

The results also indicate that edge-of-field losses from continuous corn fields would be higher than from corn–soybean fields. Furthermore, nutrient losses would be higher in fields receiving manure than in fields that do not receive manure, even though sediment losses would be lower in fields receiving manure. Judicious use of nutrients seems to play a role in these impacts, an aspect that deserves further study. Finally, the results highlight the fact that market-driven changes in producer planting decisions would likely play a role in the levels of nutrient and sediment losses under future climate projections.

Author Contributions: E.O. played the leading role in design of the research, model calibration and validation, model simulations, initial writeup, and revisions. S.H.J. contributed to data assembly, review, and revision of writeup. P.W.G. contributed to initial model calibration and validation and revision of the writeup. A.S. contributed to model calibration, validation, and testing. O.G. contributed to model setup, calibration, and testing. All authors have read and agreed to the published version of the manuscript.

Funding: Funding for a portion of this research was provided by USDA to Project No. 2012-02355 through the National Institute for Food and Agriculture's Agriculture and Food Research Initiative, Regional Approaches for Adaptation to and Mitigation of Climate Variability and Change.

Institutional Review Board Statement: Not applicable.

Informed Consent Statement: Not applicable.

Data Availability Statement: The data used for this study are all publicly available, and are cited in this paper. No restricted data were used in this paper.

Conflicts of Interest: The authors declare no conflict of interest.

References

1. Xu, Y.; Elbakidze, L.; Yen, H.; Arnold, J.G.; Gassman, P.W.; Hubbart, J.; Strager, M.P. Integrated assessment of nitrogen runoff to the Gulf of Mexico. *Resour. Energy Econ.* **2022**, *67*, 101279. [CrossRef]
2. Zeiger, S.J.; Owen, M.R.; Pavlowsky, R.T. Simulating nonpoint source pollutant loading in a karst basin: A SWAT modeling application. *Sci. Total Environ.* **2021**, *785*, 147295. [CrossRef]
3. Lerch, R.N.; Baffaut, C.; Kitchen, N.R.; Sadler, E.J. Long-Term Agroecosystem Research in the Central Mississippi River Basin: Dissolved Nitrogen and Phosphorus Transport in a High-Runoff-Potential Watershed. *J. Environ. Qual.* **2015**, *44*, 44–57. [CrossRef]
4. Carpenter, S.; Caraco, N.; Correll, D.; Howarth, R.; Sharply, A.; Smith, V. Nonpoint source pollution of surface waters with phosphorus and nitrogen. *Ecol. Appl.* **1998**, *8*, 559–568. [CrossRef]
5. Delgado, J.A.; Groffman, P.M.; Nearing, M.A.; Goddard, T.; Reicosky, D.; Lal, R.; Kitchen, N.R.; Rice, C.W.; Towery, D.; Salon, P. Conservation practices to mitigate and adapt to climate change. *J. Soil Water Conserv.* **2011**, *66*, 118A–129A. [CrossRef]
6. Hatfield, J.L.; Prueger, J.H. Impacts of changing precipitation patterns on water quality. *J. Soil Water Conserv.* **2004**, *59*, 51–58.
7. Sharpley, A.N.; Chapra, S.C.; Wedepohl, R.; Sims, J.T.; Daniel, T.C.; Reddy, K.R. Managing Agricultural Phosphorus for Protection of Surface Waters: Issues and Options. *J. Environ. Qual.* **1994**, *23*, 437–451. [CrossRef]
8. Sharpley, A.N.; Bergström, L.; Aronsson, H.; Bechmann, M.; Bolster, C.H.; Börling, K.; Djodjic, F.; Jarvie, H.P.; Schoumans, O.F.; Stamm, C.; et al. Future agriculture with minimized phosphorus losses to waters: Research needs and direction. *AMBIO* **2015**, *44* (Suppl. S2), 163–179. [CrossRef]
9. Danalatos, G.J.N.; Wolter, C.; Archontoulis, S.V.; Castellano, M.J. Nitrate losses across 29 Iowa watersheds: Measuring long-term trends in the context of interannual variability. *J. Environ. Qual.* **2022**, *51*, 708–718. [CrossRef]
10. Osei, E.; Hauck, L.; Jones, L.; Ogg, C.; Keplinger, K. *Livestock and the Environment: Lessons from a National Pilot Project*; Project Report PR0705; Texas Institute for Applied Environmental Research, Tarleton State University: Stephenville, TX, USA, 2008.
11. Macrae, M.; Jarvie, H.; Brouwer, R.; Gunn, G.; Reid, K.; Joosse, P.; King, K.; Kleinman, P.; Smith, D.; Williams, M.; et al. One size does not fit all: Toward regional conservation practice guidance to reduce phosphorus loss risk in the Lake Erie watershed. *J. Environ. Qual.* **2021**, *50*, 529–546. [CrossRef]
12. Roland, V.; Garcia, A.; Saad, D.; Ator, S.; Robertson, D.; Schwarz, G. Quantifying regional effects of best management practices on nutrient losses from agricultural lands. *J. Soil Water Conserv.* **2021**, *77*, 15–29. [CrossRef]

13. Wallace, C.W.; Flanagan, D.C.; Engel, B.A. Quantifying the effects of conservation practice implementation on predicted runoff and chemical losses under climate change. *Agric. Water Manag.* **2017**, *186*, 51–65. [CrossRef]
14. Woznicki, S.A.; Nejadhashemi, A.P. Sensitivity Analysis of Best Management Practices Under Climate Change Scenarios1. *JAWRA J. Am. Water Resour. Assoc.* **2011**, *48*, 90–112. [CrossRef]
15. Mason, R.; Merrill, S.; Görres, J.; Faulkner, J.; Niles, M. Agronomic and environmental performance of dairy farms in a warmer, wetter climate. *J. Soil Water Conserv.* **2021**, *76*, 76–88. [CrossRef]
16. Garbrecht, J.D.; Nearing, M.A.; Shields, F.D., Jr.; Tomer, M.D.; Sadler, E.J.; Bonta, J.V.; Baffaut, C. Impact of weather and climate scenarios on conservation assessment outcomes. *J. Soil Water Conserv.* **2014**, *69*, 374–392. [CrossRef]
17. Michalak, A.M.; Anderson, E.J.; Beletsky, D.; Boland, S.; Bosch, N.S.; Bridgeman, T.B.; Chaffin, J.D.; Cho, K.; Confesor, R.; Daloğlu, I.; et al. Record-setting algal bloom in Lake Erie caused by agricultural and meteorological trends consistent with expected future conditions. *Proc. Natl. Acad. Sci. USA* **2013**, *110*, 6448–6452. [CrossRef]
18. Kirchmeier-Young, M.C.; Zhang, X. Human influence has intensified extreme precipitation in North America. *Proc. Natl. Acad. Sci. USA* **2020**, *117*, 13308–13313. [CrossRef]
19. Daloğlu, I.; Cho, K.H.; Scavia, D. Evaluating Causes of Trends in Long-Term Dissolved Reactive Phosphorus Loads to Lake Erie. *Environ. Sci. Technol.* **2012**, *46*, 10650–10666. [CrossRef]
20. Jha, M.; Arnold, J.G.; Gassman, P.W.; Giorgi, F.; Gu, R.R. Climate change sensitivity assessment on Upper Mississippi River Basin streamflows using SWAT. *J. Am. Water Resour. Assoc.* **2006**, *42*, 997–1015. [CrossRef]
21. Raj, A.D.; Kumar, S.; Sooryamol, K. Modelling climate change impact on soil loss and erosion vulnerability in a watershed of Shiwalik Himalayas. *Catena* **2022**, *214*, 106279. [CrossRef]
22. Bosch, N.S.; Evans, M.A.; Scavia, D.; Allan, J.D. Interacting effects of climate change and agricultural BMPs on nutrient runoff entering Lake Erie. *J. Great Lakes Res.* **2014**, *40*, 581–589. [CrossRef]
23. O'Neal, M.; Frankenberger, J.R.; Ess, D.R.; Lowenberg-DeBoer, J. Profitability of On-Farm Precipitation Data for Nitrogen Management Based on Crop Simulation. *Precis. Agric.* **2004**, *5*, 153–178. [CrossRef]
24. Yasarer, L.M.W.; Bingner, R.L.; Garbrecht, J.D.; Locke, M.A.; Lizotte, R.E.; Momm, H.G.; Busteed, P.R. Climate Change Impacts on Runoff, Sediment, and Nutrient Loads in an Agricultural Watershedin the Lower Mississippi River Basin. *Appl. Eng. Agric.* **2017**, *33*, 379–392. [CrossRef]
25. Williams, J.R.; Arnold, J.G.; Srinivasan, R. *The APEX Model*; BRC Report No. 00-06; Blackland Research Center, Texas Agricultural Experiment Station, Texas Agricultural Extension Service, Texas A&M University System: Temple, TX, USA, 2000.
26. Williams, J.R.; Arnold, J.G.; Kiniry, J.R.; Gassman, P.W.; Green, C.H. History of model development at Temple, Texas. *Hydrol. Sci. J.* **2008**, *53*, 948–960. [CrossRef]
27. Gassman, P.W.; Williams, J.R.; Wang, X.; Saleh, A.; Osei, E.; Hauck, L.M.; Izaurralde, R.; Flowers, J.D. Invited Review Article: The Agricultural Policy/Environmental eXtender (APEX) Model: An Emerging Tool for Landscape and Watershed Environmental Analyses. *Trans. ASABE* **2010**, *53*, 711–740. [CrossRef]
28. Arnold, J.G.; Srinivasan, R.; Muttiah, R.S.; Williams, J.R. LARGE AREA HYDROLOGIC MODELING AND ASSESSMENT PART I: MODEL DEVELOPMENT. *JAWRA J. Am. Water Resour. Assoc.* **1998**, *34*, 73–89. [CrossRef]
29. Gassman, P.W.; Osei, E.; Saleh, A.; Rodecap, J.; Norvell, S.; Williams, J. Alternative practices for sediment and nutrient loss control on livestock farms in northeast Iowa. *Agric. Ecosyst. Environ.* **2006**, *117*, 135–144. [CrossRef]
30. Osei, E.; Jafri, S.H.; Saleh, A.; Gassman, P.W.; Gallego, O. Simulated Climate Change Impacts on Corn and Soybean Yields in Buchanan County, Iowa. *Agriculture* **2023**, *13*, 268. [CrossRef]
31. Gary, K.; Norvell, S.; Jones, R.; Maquire, C.; Osei, E.; Saleh, A.; Gassman, P.; Rodecap, J. *Livestock and the Environment: A National Pilot Project: CEEOT-LP Modeling for the Upper Maquoketa River Watershed, Iowa: Final Report*; Report No. PR0003; Texas Institute for Applied Environmental Research, Tarleton State University: Stephenville, TX, USA, 2000.
32. Saleh, A.; Niraula, R.; Marek, G.W.; Gowda, P.H.; Brauer, D.K.; Howell, T.A. Lysimetric Evaluation of the APEX Model to Simulate Daily ET for Irrigated Crops in the Texas High Plains. *Trans. ASABE* **2018**, *61*, 65–74. [CrossRef]
33. Tadesse, H.K.; Moriasi, D.N.; Gowda, P.H.; Marek, G.; Steiner, J.L.; Brauer, D.; Talebizadeh, M.; Nelson, A.; Starks, P. Evaluating evapotranspiration estimation methods in APEX model for dryland cropping systems in a semi-arid region. *Agric. Water Manag.* **2018**, *206*, 217–228. [CrossRef]
34. Timlin, D.; Chun, J.A.; Meisinger, J.; Kang, K.; Fleisher, D.; Staver, K.; Doherty, C.; Russ, A. Evaluation of the agricultural policy environmental extender (APEX) for the Chesapeake Bay watershed. *Agric. Water Manag.* **2019**, *221*, 477–485. [CrossRef]
35. Worqlul, A.W.; Jeong, J.; Green, C.H.M.; Abitew, T.A. The impact of rainfall distribution methods on streamflow throughout multiple elevations in the Rocky Mountains using the APEX model—Price River watershed, Utah. *J. Environ. Qual.* **2021**, *50*, 1395–1407. [CrossRef] [PubMed]
36. Cheng, G.; Harmel, R.; Ma, L.; Derner, J.; Augustine, D.; Bartling, P.; Fang, Q.; Williams, J.; Zilverberg, C.; Boone, R.; et al. Evaluation of APEX modifications to simulate forage production for grazing management decision-support in the Western US Great Plains. *Agric. Syst.* **2021**, *191*, 103139. [CrossRef]
37. Carroll, S.; Le, K.; Moreno-García, B.; Runkle, B. Simulating Soybean–Rice Rotation and Irrigation Strategies in Arkansas, USA Using APEX. *Sustainability* **2020**, *12*, 6822. [CrossRef]
38. Gautam, S.; Mbonimpa, E.G.; Kumar, S.; Bonta, J.V.; Lal, R. Agricultural Policy Environmental eXtender model simulation of climate change impacts on runoff from a small no-till watershed. *J. Soil Water Conserv.* **2015**, *70*, 101–109. [CrossRef]

39. Ford, W.; King, K.; Williams, M.; Fausey, N. Sensitivity Analysis of the Agricultural Policy/Environmental eXtender (APEX) for Phosphorus Loads in Tile-Drained Landscapes. *J. Environ. Qual.* **2015**, *44*, 1099–1110. [CrossRef]
40. Hong, E.-M.; Park, Y.; Muirhead, R.; Jeong, J.; Pachepsky, Y.A. Development and evaluation of the bacterial fate and transport module for the Agricultural Policy/Environmental eXtender (APEX) model. *Sci. Total Environ.* **2018**, *615*, 47–58. [CrossRef]
41. Kim, D.-H.; Jang, T.; Hwang, S. Evaluating impacts of climate change on hydrology and total nitrogen loads using coupled APEX-paddy and SWAT models. *Paddy Water Environ.* **2020**, *18*, 515–529. [CrossRef]
42. Kamruzzaman, M.; Hwang, S.; Choi, S.-K.; Cho, J.; Song, I.; Song, J.-H.; Jeong, H.; Jang, T.; Yoo, S.-H. Evaluating the Impact of Climate Change on Paddy Water Balance Using APEX-Paddy Model. *Water* **2020**, *12*, 852. [CrossRef]
43. Kamruzzaman, M.; Hwang, S.; Choi, S.-K.; Cho, J.; Song, I.; Jeong, H.; Song, J.-H.; Jang, T.; Yoo, S.-H. Prediction of the effects of management practices on discharge and mineral nitrogen yield from paddy fields under future climate using APEX-paddy model. *Agric. Water Manag.* **2020**, *241*, 106345. [CrossRef]
44. Bailey, R.T.; Tasdighi, A.; Park, S.; Tavakoli-Kivi, S.; Abitew, T.; Jeong, J.; Green, C.H.; Worqlul, A.W. APEX-MODFLOW: A New integrated model to simulate hydrological processes in watershed systems. *Environ. Model. Softw.* **2021**, *143*, 105093. [CrossRef]
45. Williams, J.R. The erosion-productivity impact calculator (EPIC) model: A case history. *Philos. Trans. R. Soc. B Biol. Sci.* **1990**, *329*, 421–428.
46. Saleh, A.; Gallego, O.; Osei, E.; Lal, H.; Gross, C.; McKinney, S.; Cover, H. Nutrient Tracking Tool—A user-friendly tool for calculating nutrient reductions for water quality trading. *J. Soil Water Conserv.* **2011**, *66*, 400–410. [CrossRef]
47. Edward, O.; Gassman, P.; Saleh, A. *Livestock and the Environment: A National Pilot Project: CEEOT–LP Modeling for the Upper Maquoketa River Watershed, Iowa: Technical Report*; Report No. RR0001; Texas Institute for Applied Environmental Research, Tarleton State University: Stephenville, TX, USA, 2000.
48. USDA-NASS. *USDA National Agricultural Statistics Service Cropland Data Layer*; USDA-NASS: Washington, DC, USA, 2022. Available online: https://nassgeodata.gmu.edu/CropScape/ (accessed on 21 November 2022).
49. USDA-NRCS. Soil Survey Staff, Natural Resources Conservation Service, United States Department of Agriculture. Soil Survey Geographic (SSURGO) Database. 2022. Available online: https://websoilsurvey.nrcs.usda.gov (accessed on 21 November 2022).
50. PRISM Climate Group. PRISM Climate Group, Oregon State University. 2022. Available online: https://prism.oregonstate.edu (accessed on 21 November 2022).
51. NCAR. National Center for Atmospheric Research: Earth System Grid Portal, Climate Data Gateway. 2022. Available online: https://www.earthsystemgrid.org/ (accessed on 21 November 2022).
52. Monaghan, A.J.; Steinhoff, D.F.; Bruyere, C.L.; Yates, D. NCAR CESM Global Bias-Corrected CMIP5 Output to Support WRF/MPAS Research. Research Data Archive at the National Center for Atmospheric Research, Computational and Information Systems Laboratory. 2014. Available online: https://doi.org/10.5065/D6DJ5CN4 (accessed on 11 June 2017).
53. IPCC. *Climate Change 2013: The Physical Science Basis. Contribution of Working Group I to the Fifth Assessment Report of the Intergovernmental Panel on Climate Change*; Stocker, T.F., Qin, D., Plattner, G.-K., Tignor, M., Allen, S.K., Boschung, J., Nauels, A., Xia, Y., Bex, V., Midgley, P.M., Eds.; Cambridge University Press: Cambridge, UK; New York, NY, USA, 2013; p. 1535. Available online: https://www.ipcc.ch/site/assets/uploads/2018/02/WG1AR5_all_final.pdf (accessed on 28 July 2022).
54. Taylor, K.E.; Stouffer, R.J.; Meehl, G.A. An Overview of CMIP5 and the Experiment Design. *Bull. Am. Meteorol. Soc.* **2012**, *93*, 485–498. [CrossRef]
55. Coffey, R.; Paul, M.J.; Stamp, J.; Hamilton, A.; Johnson, T. A Review of Water Quality Responses to Air Temperature and Precipitation Changes 2: Nutrients, Algal Blooms, Sediment, Pathogens. *JAWRA J. Am. Water Resour. Assoc.* **2019**, *55*, 844–868. [CrossRef]
56. USEPA. EnviroAtlas Data Download. National Table Downloads. 2022. Available online: https://www.epa.gov/enviroatlas/forms/enviroatlas-data-download (accessed on 11 November 2022).
57. Sangchul, L.; Sadeghi, A.M.; Yeo, I.-Y.; McCarty, G.W.; Hively, W.D. Assessing the Impacts of Future Climate Conditions on the Effectiveness of Winter Cover Crops in Reducing Nitrate Loads into the Chesapeake Bay Watersheds Using the SWAT Model. *Am. Soc. Agric. Biol. Eng.* **2017**, *60*, 1939–1955. [CrossRef]
58. Li, T.; Zhang, Y.; He, B.; Wu, X.; Du, Y. Nitrate loss by runoff in response to rainfall amount category and different combinations of fertilization and cultivation in sloping croplands. *Agric. Water Manag.* **2022**, *273*, 107916. [CrossRef]